Fusion Engineering and Design 192 (2023) 113614

Contents lists available at ScienceDirect

Fusion Engineering and Design

journal homepage: www.elsevier.com/locate/fusengdes

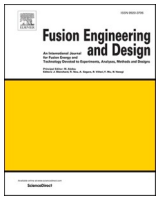

A double-ended helicon source to symmetrize RAID plasma

R. Jacquier *, R. Agnello, M. Baquero-Ruiz, H. Bergerioux, Ph. Guittienne, A.A. Howling, L. Kadi, R. Karimov, C. Stollberg, S. Vincent, I. Furno

Ecole Polytechnique Fédérale de Lausanne (EPFL), Swiss Plasma Center (SPC), CH-1015 Lausanne, Switzerland

ARTICLE INFO

Keywords:
RAID
Plasma
Source
RF
Helicon
Antenna
Wave
Negative ions
Langmuir
RF compensation

Neutral Beam Injectors (NBI) for post-DEMO-like reactors must achieve a neutralization efficiency (fraction neutrals/ions) above 70%. To reach this, NBIs based on negative ions are necessary and an innovative concept of this type of injector is based on photo-neutralization. In this context, RAID (Resonant Antenna Ion Device), a linear helicon system located at the Swiss Plasma Center (SPC) in the Ecole Polytechnique Fédérale de Lausanne (EPFL), aims to study the production of negative ions (D^- and H^-) in the plasma volume.

RAID is routinely operated with a single resonant birdcage antenna, located on one end of the vacuum chamber (1.4 m long and 40 cm diameter) at 0.3 Pa of pressure in D_2 and H_2 discharges. This antenna, excited at 13.56 MHz with a RF power up to 10 kW, generates helicon driven plasma beams extending all along the chamber when a DC axial magnetic field (standard value 200 G) is applied. Typical electron densities at the center of the column are 1–2.5 $\times$ 10^{18} m^{-3} and the electron temperature of 4–6 eV. In order to improve the symmetry as well as the homogeneity of plasma parameters along the axis, a second source was installed at the opposite end of the vacuum vessel and a complementary coil for the DC magnetic field was added. Axial profiles and 2D mappings of plasma density and temperature have been measured with a Double Langmuir Probe (DLP). Interestingly, for most phases, the relative RF phase of the two antennas influences the plasma causing very low frequency (few Hz) beating. In the future, other plasma diagnostics will be developed such as Thomson scattering, LIF (Laser Induced Fluorescence) and B-dot measurements to characterize in detail the wave propagation in RAID with two antennas and to understand better some phenomena observed during the test campaign described in this article.

1. Introduction

Neutral Beam Injectors (NBI) for ITER-like reactors must be able to produce and accelerate deuterium neutrals with energy of the order of 1 MeV [1,2]. For such energy, the well-known technology of positive ion NBI would not provide a sufficient neutralization efficiency, defined as the ratio between the power flux of neutral particles at the exit of the neutralizer and that of the ions at the entrance; negative ion NBI will be required [1,2]. While in the EuroFusion program, the photo-neutralizer is no longer considered for DEMO due to an insufficient Technology Readiness Level, research is still conducted for a post-DEMO device. In a photo-neutralization based neutralizer, one conceptual design of injectors foresees to extract negative ions D^- from a 3 m long and 15 cm wide plasma, and to photo-neutralize the accelerated negative ions [3,4]. Thereby, a plasma source able to generate homogeneous and dense plasmas on such area has to be developed.

In this context, as an alternative to standard inductively coupled plasmas (ICPs), helicon plasma sources have been proposed. These may have advantages when compared to ICP plasma sources: 1) At low pressure ($<$ 0.3 Pa), when the RF wave damping is weak, helicon plasmas provide a quasi-homogeneous electron density along the plasma column generated, resulting in a geometry which fits the shape of the conceptual design. 2) For the same RF power, the helicon mode typically provides an electron density one order of magnitude higher than the inductive mode. Previous interferometric measurements have shown a density of 10^{18} m^{-3} inside the plasma column, for hydrogen and deuterium [4]. However, the mechanisms of power deposition of the helicon waves still require further investigation. 3) The radial electron temperature profile, which is in the order of 6 to 10 eV in the center and drops to 1 eV in the periphery (around 5 cm from the center), is favorable to populate the vibrational states of H_2 or D_2 molecules in the hot area and to enhance the dissociative attachment of electrons in the cold periphery.

RAID, the Resonant Antenna Ion Device, is a linear helicon plasma

* Corresponding author.
E-mail address: remy.jacquier@epfl.ch (R. Jacquier).

https://doi.org/10.1016/j.fusengdes.2023.113614
Received 13 October 2022; Received in revised form 30 January 2023; Accepted 27 February 2023
Available online 10 March 2023

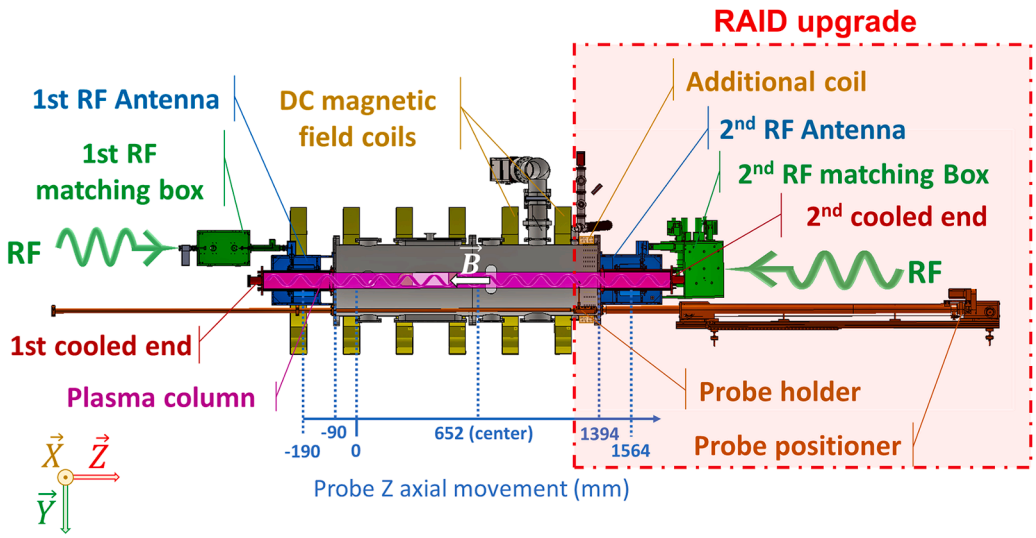

Fig. 1. RAID device and auxiliaries.

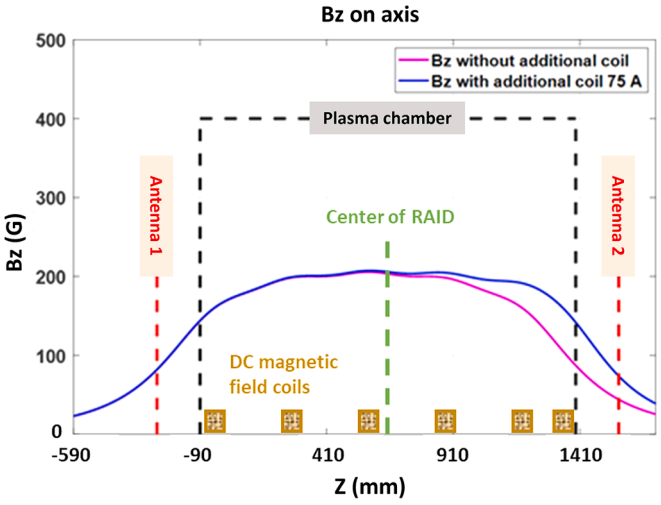

Fig. 2. Intensity of the axial component of the DC magnetic field in the twin antennas configuration.

device located at the Swiss Plasma Center (SPC) dedicated to the study of the volume production of negative ions (H^- and D^-) in helicon plasmas [3]. Up to date, investigations on RAID were conducted in the presence of a single resonant antenna in a birdcage geometry, located on one end of the vacuum chamber. In this configuration, while the axial electron density is quasi-homogeneous axially, the electron temperature decreases along the axis of the device moving away from the resonant antenna [3–6].

In this paper, a twin resonant antenna has been added on the opposite end of the plasma chamber to improve the axial profile of the electron temperature and increase the total power coupled to the plasma. Furthermore, an additional DC magnetic field coil has been

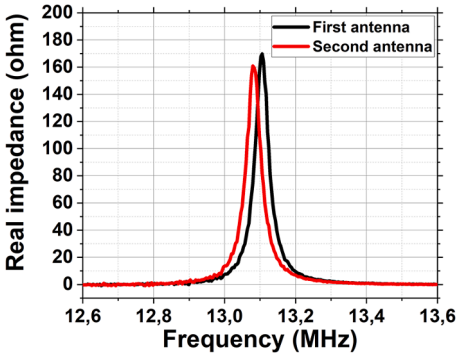

Fig. 4. Input impedance of each birdcage antenna.

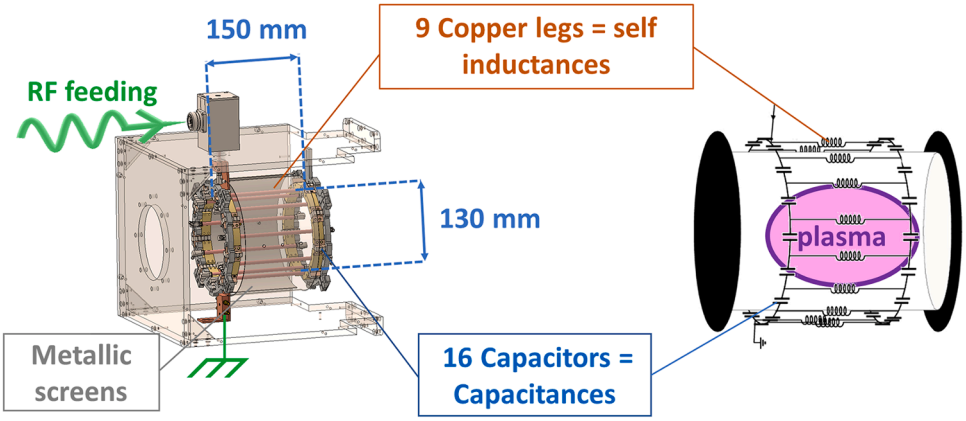

Fig. 3. RAID birdcage antenna.

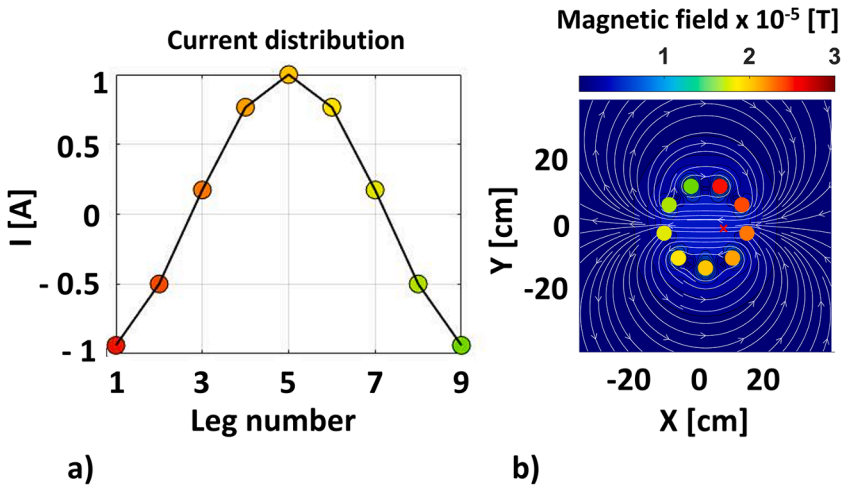

Fig. 5. Normalized current distribution in the RAID birdcage antenna on a) and the resulting magnetic field lines on b). Both are given at one instant in time.

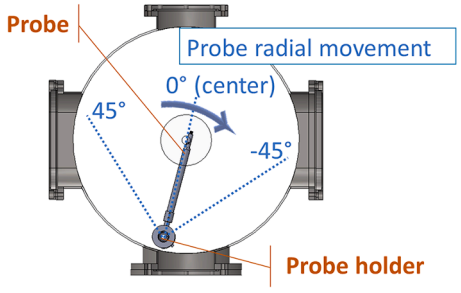

Fig. 6. Raid cross section and radial movement of the probe.

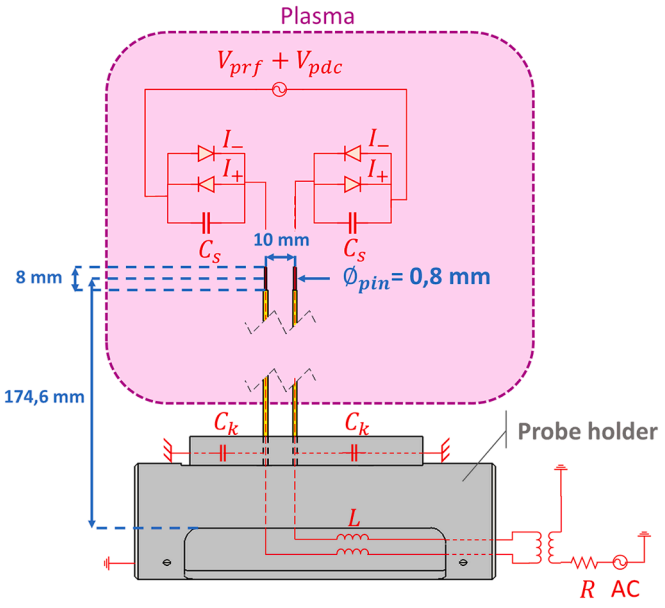

Fig. 7. RAID Double Langmuir Probe geometry and electric scheme.

installed on the new antenna side, to render the magnetic field symmetric with respect to the center of the device. Finally, a Double Langmuir Probe (DLP), installed on a newly designed 2D positioner, has been used to characterize the plasma.

The RAID device is detailed in Section 2. The new DLP is described in Section 3. In Section 4 we show measurements performed on RAID

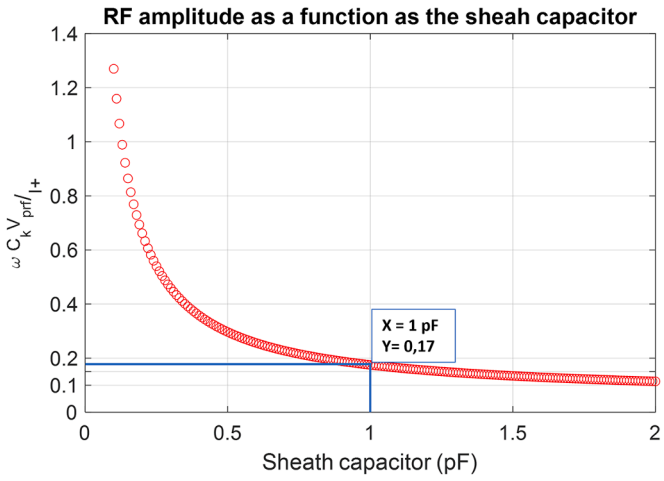

Fig. 8. The $\omega C_k V_{prf}/I_+$ criterion as a function of the sheath capacity.

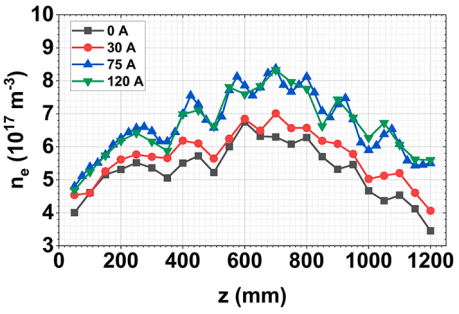

Fig. 9. Effect of the additional DC magnetic field coil on n_e profiles. Measurement profiles are on-axis and the plasma is generated in a twin antenna configuration in H_2 plasmas, pressure = 0.3 Pa, on-axis B_{field} = 200 G, power = 1.5 kW per source.

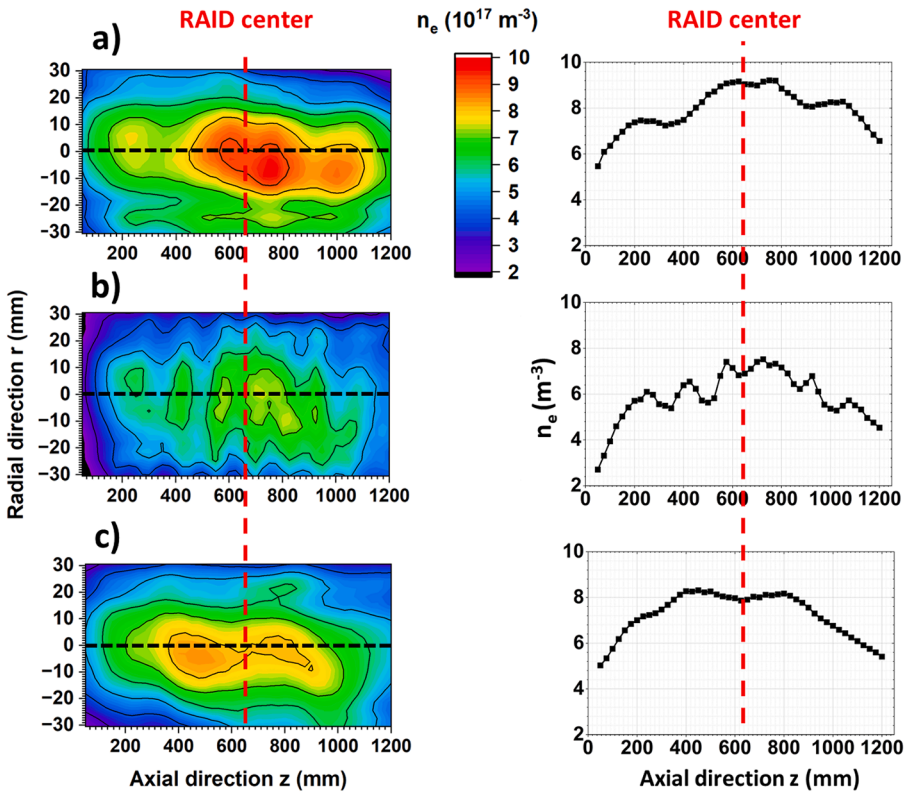

Fig. 10. 2D mappings (left column) and on-axis profiles (right column) of RAID electron temperature. a) Left antenna only, b) two twin antennas c) right antenna only.

typical plasmas. Finally, conclusions are presented in Section 5 together with a brief outlook of future research on RAID.

2. Resonant antenna ion device (RAID)

2.1. Design, configuration and upgrades

Fig. 1 details the main elements of the RAID experimental set up and further information can be found in Ref [3]. The cylindrical stainless steel main chamber is approximately 1.5 m long and 40 cm in diameter. A turbomolecular pump maintains a chamber base pressure of 1×10^{-4} Pa while the gas pressure in plasma discharges is maintained from 0.1 Pa to 1.5 Pa. A gas control panel can select different gases among H_2, D_2, He, Ne, O_2 and Ar in order to inject a constant flow of a few tens of sccm into the chamber. DC coils surround the vacuum vessel and generate a uniform magnetic field on-axis up to 660 G (0–510 A in the main DC field coils). Fig. 2 shows the axial magnetic field with the additional DC magnetic field coil of 0.51 m diameter and 32 turns located around $z \approx$ 1.4 m. To reach B_{field} uniformity in the chamber and to homogenize the field in the second antenna region, the current in the additional coil has been set to 75 A.

The twin antennas are installed on the end flanges (Fig. 1). RF generators, automatic matching boxes (in a T-matching configuration) and transmission lines are identical for both sources and designed to deliver up to10 kW of RF power with a minimum of reflected power when a real impedance of 50 ohm is matched. Although the alumina end tubes, end plates and the chamber are actively cooled to sustain the plasma heat load, the system has not yet been powered above 5 kW per source in a double antenna configuration to be conservative with diagnostics inserted in the plasma core.

2.2. Birdcage resonant antenna

The birdcage antennas are shown schematically in Fig. 3. High RF resonant currents in the copper tube legs have made this antenna an interesting ICP source, first proposed in Ref. [7] and then developed and characterized at the SPC.

As shown in Fig. 3, RAID birdcages are 130 mm in diameter, 150 mm long and are made of a mesh of capacitors and inductors. Capacitors are commercial SMD components with high Q factor. Ten of them are assembled in parallel to obtain a total capacitance of 4 nF and to sustain currents up to 150 A rms or a voltage of 1000 V rms. Inductors are water-cooled copper tubes, called copper legs in Fig. 3. The resulting antennas have N-1 modes (m) of resonance (N = 9 is the number of legs) and are excited at 13.56 MHz at a typical mode m = 1 [8]. The impedance spectrum in vacuum of both antenna networks for this mode are shown in Fig. 4 and a simulation of the resulting azimuthal current distribution is shown in Fig. 5(a).

Note that without DC magnetic field, birdcages can ignite pure inductive plasmas, which diffuse slightly due to the low pressures, but are concentrated in the source area. Depending on the plasma coupling, birdcage sources dissipate power into the plasma, resulting in a drop of the resonance impedance and a shift of the resonance frequency. Two cylindrical metal screens, acting as current mirrors, can be manually moved to vary their distance from antenna and are used to finely adjust the resonance frequency. In the twin configuration, both screens are tuned to have a similar resonance around 13.1 MHz (Fig. 4) without plasma coupling. With plasma this resonance will then shift to the required 13.56 MHz, as explained in Ref. [8–10].

2.3. Propagation of helicon waves with a birdcage antenna

In RAID, when helicon waves propagate, a dense plasma column of around 10 cm diameter (depending on RF power and DC magnetic field)

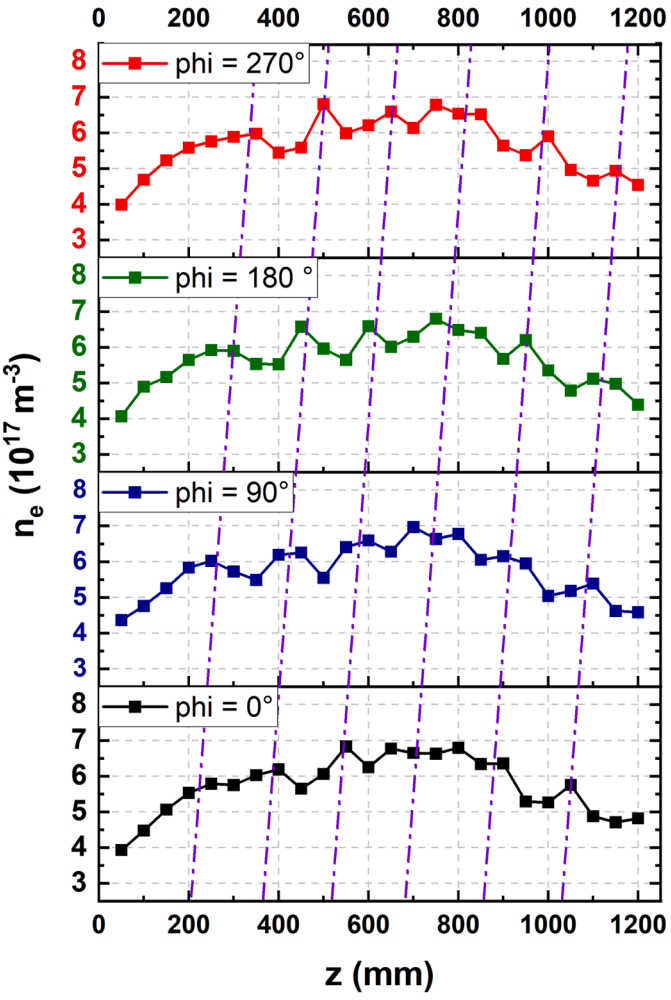

Fig. 11. RAID electron density while moving the phase between the two generators. Measurement profiles are on-axis and the plasma is generated in a twin antenna configuration in H_2 plasmas, pressure = 0.3 Pa, On-axis B_{field} = 200 G, power = 1.5 kW per source.

is visible through the glass windows and reaches the water-cooled end plates labeled on Fig. 1.

Fig. 5(b) shows the inner transverse RF magnetic field of a birdcage induced by the azimuthal current distribution on Fig. 5(a), at the specific mode of birdcage resonance m = 1. In the presence of an external axial DC magnetic field (normal to the plane X/Y of Fig. 5(b)) created by the Helmholtz coils (Figs. 1 and 2), this RF magnetic field efficiently excites helicon waves, a category of bounded whistler waves propagating in magnetized plasma medium [7,11]. According to the simple plane wave dispersion for helicon waves in an infinite plasma described by Boswell [11], the wavelength depends on electron density and on axial DC magnetic field. This last point explains the need to uniformize the DC magnetic field with the additional DC coil.

3. RAID Double Langmuir Probe (DLP)

To characterize RAID plasmas, a Double Langmuir Probe (DLP) was installed on the probe holder, moving in 2D inside the chamber. Its axial movement is shown in Fig. 1, while Fig. 6 shows the radial movement. The current driven by a DLP is always limited by the ion saturation current, this results in an extended lifetime compared to a standard Single Langmuir Probe (SLP) and reduced perturbation to the plasma. Ion dynamics are also much less affected by DC magnetic fields, resulting in a more accurate analysis of the I/V curves. The standard opinion is that DLPs are by default RF compensated because, theoretically, they float with the plasma potential fluctuations. Nevertheless, self-bias can appear on probe tips due to RF fluctuations as described by Caneses et al. [12]. In this recent article, the authors explain that the DLP level of RF compensation can be characterized by the following criterion:

$$\omega C_k \frac{V_{prf}}{I_+} \ll 1. \quad (1)$$

where $\omega = 2\pi f$ is the RF angular frequency, C_k is the stray capacitance of the probe, V_{prf} is the amplitude of the RF plasma potential (while V_{pdc} in Fig. 7 is the DC part) and I_+ is the ion saturation current. On Fig. 7, C_s is the sheath capacitance of the Langmuir probe and together with C_k, they depend on the probe geometry and they especially affect the RF compensation. In H_2 plasmas at 0.3 Pa with two antennas and 200 G of DC magnetic field, the electron density in the central column of RAID is approximately 5×10^{17} m^{-3}. In such conditions, $C_s \approx 1$ pF, $I_+ = 0.04$ A, $V_{prf} \approx 16$ V and $\omega C_k V_{prf}/I_+ = 0.17$ (Fig. 8).

With $\omega C_k V_{prf}/I_+ = 0.17$, following Fig. 4 of Ref. [12] the error on V_{float} is expected to be below 0.5 V with no impact on T_e measurements and only a small uncertainty on n_e. Because the criterion depends inversely on I_+, the error would increase significantly while going towards the edges of the column where densities are lower.

A schematic of the DLP designed and built for RAID is shown in Fig. 7. The DLP is composed of two tantalum tips (8 mm length and 0.8 mm diameter) covered by alumina tubes to insulate the rest of the wire from the plasma. The choice of tantalum was dictated by a reduced sputtering on the probe tips in Ar plasmas, thus significantly improving the tips lifetime. The two tips are 10 mm apart and they cross the center of the plasma column at 174.6 mm from the probe holder axis. Each of the double tip signals passes through a choke of 230 μH and is connected to the floating secondary of a transformer. The primary is connected to the applied bias potential (triangular waveform) and to the current measurement giving the I/V curve with a sweep of 47 Hz. Higher frequency can induce hysterical behaviors. This DLP was used for all the following measurements of electron density and temperature.

4. DLP profiles measurements

4.1. Uniformization of the DC magnetic field

The DC magnetic field in RAID axis was computed in Matlab (Fig. 2) to simulate the additional coil (see Fig. 1), to adjust its position and the coil current to have the same magnetic field at both antenna locations.

The effect of the additional DC magnetic field coil on n_e profiles is shown in Fig. 9. The most symmetric and dense n_e profiles are observed with 75 A current in the additional coil. Below this value, n_e becomes asymmetric, the presence of a divergent DC magnetic field where the second antenna is located affects the propagation of the helicon wave and the resulting plasma density on the right side of Fig. 9 is lower. Moreover, the density of the entire axial profile decreases when the additional coil has a current below 75 A. The DC magnetic field in the second antenna region (Fig. 2) might start to be not sufficient to propagate the wave with a coupling in between magnetized (helicon excitation) and non-magnetized (ICP excitation).

4.2. Profiles with different antenna configurations

To improve the axial homogeneity of plasma parameters and to test the new configuration dedicated to high density plasmas, comparisons have been performed between one antenna on the right end only, one antenna on the left end only, and finally with both antennas (Fig. 1).

The plasma for this test campaign is a hydrogen discharge with a pressure of 0.3 Pa (during the discharge). The DC magnetic field current is set to 150 A and to 75 A in the additional coil to obtain a DC magnetic

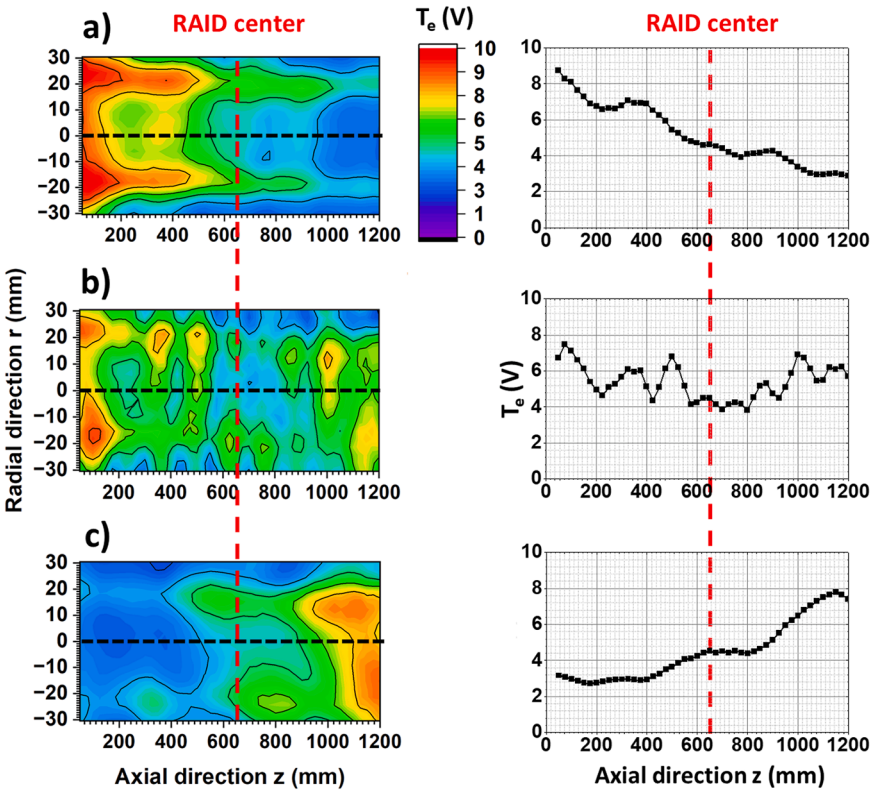

Fig. 12. 2D mappings (left column) and on-axis profiles (right column) of RAID electron temperature. a) Left antenna only, b) two twin antennas c) right antenna only.

field around 200 G on-axis. The RF delivered power is maintained at 3 kW when only one antenna is running (Figs. 10(a,c) and 12(a,c)) and 1.5 kW per antenna with the twin antenna configuration (Fig. 10(b) and 12(b)) to have a comparable total power deposited in the plasma. With such parameters, H_2 plasmas are quite stable and no significant crosstalk between antennas is observed, which could otherwise perturb the impedance matching of either resonant antenna. Both RF generators share the same clock and the identical frequency is set to 13.56 MHz while the phase between the two antenna RF sources is arbitrarily set to 90°

Fig. 10 summarizes the electron density measured in RAID in the different configurations. The density profiles of the single antenna cases (Fig. 10(a,c)) are very similar with a variation of ~10%. A modulation with a wavelength of ~240 mm can be seen and corresponds to the 240 mm wavelength of the helicon standing wave evidenced in previous B-dot measurements [13,14]. For the two antennas case (Fig. 10(b)), the absolute density is lower by ~ 20% and a modulation at 100 - 120 mm is observed, which agrees with an interference of the standing waves of the twin sources.

Fig. 11 shows how this standing wave pattern moves axially by varying the phase between the two RF generators. For unknown reasons, between 0 and 200 mm, there are no oscillations whereas the standing wave shifts along the rest of RAID axis. During these measurements, for some phases the plasma was unstable and the discharge was beating at a very low frequency (few Hz), whereas for some other the plasmas were completely stable. This effect is probably due to constructive/destructive interferences of the two antenna waves, but more experiments are required to investigate this assumption.

Fig. 12 summarizes the electron temperature measured in RAID with the same configurations. The temperature decreases by approximately 2/3 along the plasma column for single antenna cases (Fig. 12(a,c)). For the two antennas configuration (Fig. 12(b)), the temperature profile is more symmetric and homogeneous, even if an inhomogeneity remains due to the quite strong modulation already observed on n_e.

In Section 4, $\omega C_k V_{prf}/I_+ = 0.17 < 1$ has been calculated and with such values, according to Caneses et al. [12] the DLP should be RF compensated. Following the same reference, an insufficient RF compensation on DLP in RAID range of plasma parameters might lead to an overestimation of n_e but would not influence the T_e. In measurements reported in this article, there is a clear modulation on both n_e and T_e axial profiles, at a wavelength apparently comparable to the helicon standing wave. This modulation could be a physics phenomenon and the plasma parameters could effectively follow the standing wave of the helicon wave. Nevertheless, one could also fairly question the validity of the RF compensation due to the habitual distortion of I/V curves of SLP in RF plasmas [15].

5. Conclusions

We reported on a major RAID upgrade comprising the installation of a second helicon resonant antenna and an additional magnetic field coil. This resulted in an improvement of the symmetry and the homogeneity of T_e along the axis. However, the symmetry of n_e can be improved by finely adjusting the DC magnetic field, which plays an essential role in helicon wave propagation, by adjusting the power on each antenna and also by adjusting the phase between the RF feeding of the twin antennas. In this case, a visible emission beating appears as well as a small crosstalk between the twin RF sources, which is nevertheless well managed and filtered by the automatic matching.

A DLP probe has been designed, built and tested, obtaining first promising measurements. However, some open questions remain. The wavelength of 240 mm seen on the modulation of T_e and n_e consistent with the helicon standing wave measured in previous campaigns could also be a sign of an insufficient RF compensation. If it is a real effect, it may be detrimental to beam divergency when negative ions are extracted and the issue will have to be addressed.

The next step will be to install a B-dot probe to characterize the helicon wave RF magnetic field with one or two sources. This will provide a better understanding of the helicon wave propagation and of the processes of high energy deposition that are involved in the helicon plasma generation. The physical aspects of the interaction between two waves driven by two independent helicon sources will also be explored. In parallel, new diagnostics such as LIF (Laser Induced Fluorescence) and TALIF (Two-Photon Absorption Laser Fluorescence), Thomson scattering and microwave interferometry will be implemented for complementary measurements of T_e, n_e, and T_i. With the described upgrade, RAID also represents a prototype for a long multi-antenna system to be investigated for generating dense and uniform plasmas for elongated plasma sources such as AWAKE at CERN and can thus contribute to research in the domain of wakefield acceleration using helicon plasmas.

Declaration of Competing Interest

The authors declare that they have no known competing financial interests or personal relationships that could have appeared to influence the work reported in this paper.

Data availability

Data will be made available on request.

Acknowledgments

This work has been carried out within the framework of the EUROfusion Consortium, partially funded by the European Union via the Euratom Research and Training Programme (Grant Agreement No 101052200 — EUROfusion). The Swiss contribution to this work has been funded by the Swiss State Secretariat for Education, Research and Innovation (SERI). Views and opinions expressed are however those of the author(s) only and do not necessarily reflect those of the European Union, the European Commission or SERI. Neither the European Union nor the European Commission nor SERI can be held responsible for them.

References

[1] P. Sonato, et al., Conceptual design of the beam source for the DEMO neutral beam injectors, New J. Phys. 18 (2016), 125002.
[2] A. Simonin, et al., Negative ion source development for a photoneutralization based neutral beam system for future fusion reactors, New J. Phys. 18 (2016), 125005.
[3] I. Furno, et al., Helicon wave-generated plasmas for negative ion beams for fusion, EPJ Web of Conferen. 157 (2017) 03014.
[4] R. Agnello, Thesis (PHD), EPFL n°7817. Negative hydrogen ions in a helicon plasma source, 2020.
[5] R. Agnello, et al., Cavity ring-down spectroscopy to measure negative ion density in a helicon plasma source for fusion neutral beams, Rev. Sci. Instrum. 89 (2018), 103504.
[6] R. Agnello, et al., Negative ion characterization in a helicon plasma source for fusion neutral beams by cavity ring-down spectroscopy and Langmuir probe laser photodetachment, Nucl. Fusion. 60 (2020), 026007.
[7] Ph. Guittienne, et al., Towards an optimal antenna for helicon waves excitation, J. Appl. Phys. 98 (2005), 083304.
[8] Ph. Guittienne, et al., Analysis of resonant planar dissipative network antennas for rf inductively coupled plasma sources, Plasma Sources Sci. Technol. 23 (2014), 015006.
[9] A.A. Howling, et al., Complex image method for RF antenna-plasma inductive coupling calculation in planar geometry. Part I: basic concepts, Plasma Source. Sci. Technol. 24 (2015), 065014.
[10] Ph. Guittienne, et al., Complex image method for RF antenna-plasma inductive coupling calculation in planar geometry. Part II: measurements on a resonant network, Plasma Source. Sci. Technol. 24 (2015), 065015.
[11] R.W. Boswell, Very efficient plasma generation by whistler waves near the lower hybrid frequency, Plasma Phys. Control. Fusion. 26 (1984) 1147.
[12] J.F. Caneses, et al., RF compensation of double Langmuir probes: modelling and experiment, Plasma Sources Sci. Technol. 24 (2015), 035024.
[13] R. Jacquier, et al., First B-dot measurements in the RAID device, an alternative negative ion source for DEMO neutral beams, Fusion Eng. Des. 146 (2019) 1140–1144.
[14] Ph. Guittienne, et al., Helicon wave plasma generated by a resonant birdcage antenna: magnetic field measurements and analysis in the RAID linear device, Plasma Source. Sci. Technol. 30 (2021), 075023.
[15] I.D. Sudit, F.F. Chen, RF compensated probes for high-density discharges, Plasma Source Sci. Technol. 3 (1994) 162.